

Preliminary Results on the Use of Transmitarrays in 5G Antenna Systems

*Original*

Preliminary Results on the Use of Transmitarrays in 5G Antenna Systems / Beccaria, M., Massaccesi, A., Pirinoli, P.. - (2018). (2018 IEEE MTT-S International Wireless Symposium (IWS) Chengdu, China 6-10 May 2018) [10.1109/IEEE-IWS.2018.8400793].

*Availability:*

This version is available at: 11583/2710329 since: 2021-01-25T15:42:44Z

*Publisher:*

IEEE

*Published*

DOI:10.1109/IEEE-IWS.2018.8400793

*Terms of use:*

This article is made available under terms and conditions as specified in the corresponding bibliographic description in the repository

*Publisher copyright*

IEEE postprint/Author's Accepted Manuscript

©2018 IEEE. Personal use of this material is permitted. Permission from IEEE must be obtained for all other uses, in any current or future media, including reprinting/republishing this material for advertising or promotional purposes, creating new collecting works, for resale or lists, or reuse of any copyrighted component of this work in other works.

(Article begins on next page)

# Preliminary Results on the Use of Transmitarrays in 5G Antenna Systems

Michele Beccaria, Andrea Massaccesi, Paola Pirinoli  
Dept. of Electronics and Telecomm. Politecnico di Torino  
Torino, Italy

[michele.beccaria@polito.it](mailto:michele.beccaria@polito.it), [andrea.massaccesi@polito.it](mailto:andrea.massaccesi@polito.it), [paola.pirinoli@polito.it](mailto:paola.pirinoli@polito.it)

**Abstract**— In this paper, preliminary results on the feasibility of a multibeam antenna based on the use of a transmitarray are presented. Two different configurations are considered, adopting a different type of unit-cell. Their analysis proves that TA are potentially good candidates for this application, even if an optimization of the structure could be useful to improve the antenna performances.

**Keywords**—5G mobile communication, Transmitarray antenna, massive multiple-input multiple-output (MIMO), Beamscanning.

## I. INTRODUCTION

The next 5th Generation (5G) of communication systems is expected to reach a very high data rate (Gb/s), corresponding to a 1000 times faster communication compared to the current technology [1]. In order to satisfy such impressive data traffic requirements [2], a notable effort in the research and exploration of novel and revolutionary technologies is needed. From the antenna point of view, particular attention is devoted to the design of multibeam antennas [3], [4], able to radiate several independent, high gain beams covering different angular regions. In this way, the main limitations of a single beam configuration, as the inability to serve multiple users or the difficulty in covering the communication paths that are not on the line of sight, can be overcome.

Moreover, multibeam antennas represent the enabling technology for the realization of massive Multiple-Input Multiple-Output (MIMO) architectures, often designed to work in the unutilized millimeter wave (mm-wave) bands [4]-[6] or in the unlicensed  $\mu$ wave bands. A wide overview of the existing multibeam antenna technologies is provided in [7], including different phased arrays, beamforming circuits and various analog/digital phase shifting methods. Among the others, in [7] also Transmitarrays (TAs) are considered as possible candidate for the realization of efficient multibeam antennas.

Transmitarrays are considered one of the most promising solutions for the realization of high gain, low cost and high efficiency antennas. They are similar to lenses, since they behave as these devices, but with the difference that they are planar and their surface is discretized by unit-cells with size lower or equal to  $\lambda_0/2$ , being  $\lambda_0$  the wavelength at the design frequency  $f_0$  [8]. The phase of the incident field is properly adjusted acting on one or more geometrical parameters of the unit-cell: it can consist of several layers of elements printed on dielectric substrates [9], perforated dielectric elements [10], or

a combination of both techniques [11]. Transmitarray working principle is close to that adopted by reflectarrays; nevertheless, since TAs are transmitting devices, they do not suffer for the blocking of the feed, that can be centered and located closer to TA surface: the resulting structure is therefore more compact than a reflectarray antenna. Transmitarrays can be adopted in a wide range of applications [8], and recently some results have also been presented on their use in multibeam massive MIMO systems [13].

With this application in mind, in this paper two possible configurations for the realization of multibeam TAs are investigated. They differ for the type of adopted unit-cell: the first one consists of three dielectric layers with the same Malta-cross patch printed on each of them; the second unit-cell is a completely dielectric structure, made-up of three layers: in the central one there is a square hole, while in the external two the identical holes have a truncated pyramid shape. After a description of the two unit-cells, the results of their application to the design of two square TAs, with the same electrical size  $D = 10\lambda_0$  and the same  $F/D$  are presented and compared.

## II. TA UNIT-CELLS

In this section, the two considered TA unit-cells are introduced and analyzed.

### A. Malta-cross based TA unit-cell

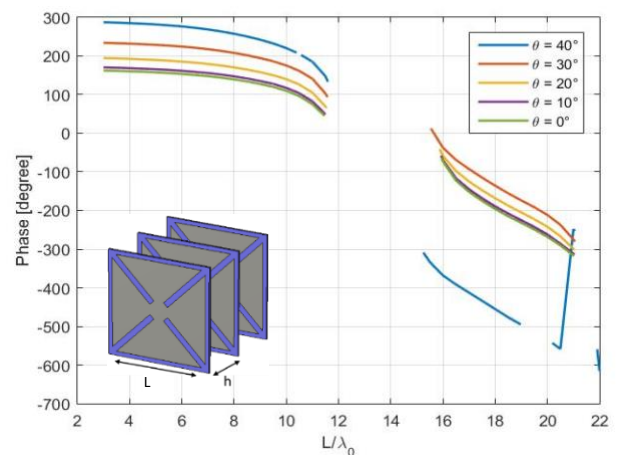


Fig. 1 - Malta-cross based unit-cell: variation of the  $S_{21}$  phase with  $L/\lambda_0$  computed for different angles of incidence. Inset: sketch of the unit-cell.

This activity is funded by the General Directorate for Cultural and Economic Promotion and Innovation of the Ministry of Foreign Affairs and International Cooperation, of the Italian Republic.

The first unit-cell consists of three overlapping dielectric layers, with the same Malta-cross patch printed on each of them. This type of element is chosen in view of its good performances especially for what concerns the bandwidth; despite to what is proposed in [15], where Malta-crosses are applied to the design of a reflectarray and both their size  $L$  and the length of the slots are used to control the re-radiating element phase, here the only free parameter is  $L$ . The adopted material has a dielectric constant  $\epsilon_r = 2.57$ ; its thickness, and the spacing between two following layers are chosen in such a way that the total distance between two printed elements is almost  $\lambda_0/4$  at the design frequency. The unit-cell size is  $\lambda_0/2$ , in order to avoid grating lobes.

A sketch of the unit cell is shown in the inset of Fig. 1, where the variation of the phase of  $S_{21}$  with  $L/\lambda_0$ , considering different incidence angles, is plotted: as it can be seen the phase range is greater than  $360^\circ$  but the curves present some discontinuities: this is due to the fact that for some values of the geometrical parameter higher order modes occur, and the magnitude of  $S_{21}$  decreases. To avoid it reduces too much, the values of  $L$  corresponding to an amplitude of  $S_{21}$  lower than -1 dB are discarded, and the discontinuous curves plotted in Fig. 1 for its phase and in Fig. 2 for its amplitude, are obtained. The unit-cell characterization has been done considering it embedded in a periodic structure and carrying out simulations with CST Microwave Studio.

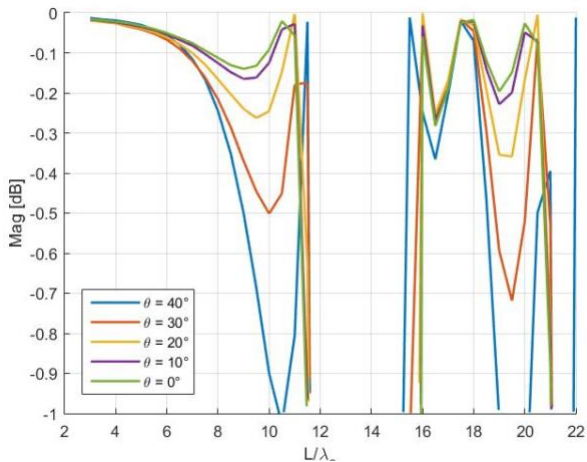


Fig. 2. Malta-cross based unit-cell: variation of the  $S_{21}$  amplitude with  $L/\lambda_0$  computed for different angles of incidence.

### B. Perforated Dielectric TA unit-cell

The second unit-cell is a triple-layer, perforated dielectric structure: the central layer is characterized by a square hole, while the two external elements present a truncated pyramid hole, as shown in Fig. 3. They act as matching layers and have been added to improve the bandwidth of the unit-cell exploiting the tapered matching concept [16]. The phase of the incident field is instead controlled changing the hole size  $d$ . The dielectric material is RT Duroid 6006, that has a permittivity of  $\epsilon_r = 6.15$

and  $\tan\delta = 0.0027$ . The unit-cell periodicity is  $W = \lambda_0/4$ , while its total thickness is  $T = \ell_1 + 2\ell_2 = 1.35\lambda_0$ .

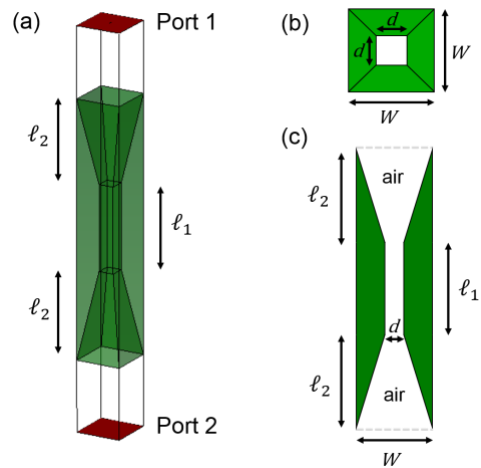


Fig. 3. Perforated dielectric TA unit-cell with tapered matching layers: (a) 3D view of the CST model. (b) Top view. (c) Side view.

The dielectric structure has been simulated using CST Microwave Studio, using periodic boundaries. The amplitude and phase variation of the transmission coefficient with  $d/\lambda_0$  and considering different incidence angles, are shown in Fig. 4 and Fig. 5, respectively. Fig. 4 proves that the matching layers provide a value of the  $S_{21}$  magnitude never worse than -1 dB. The obtained  $S_{21}$  phase range is greater than  $360^\circ$ , as pointed out in Fig. 5. Changing the angle of incidence, the phase curves stay almost parallel and do not present discontinuities.

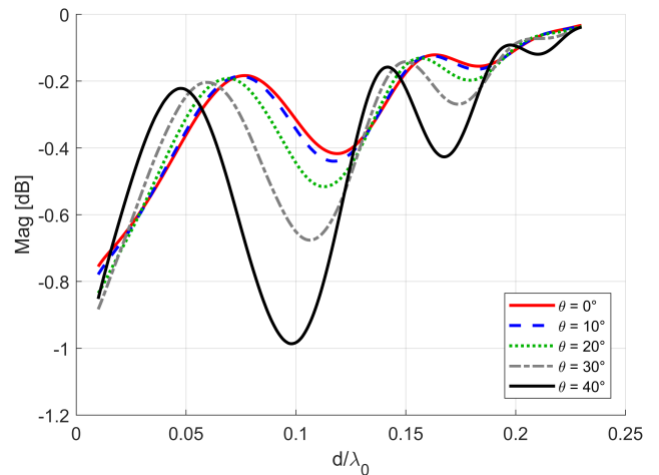


Fig. 4. Perforated dielectric unit-cell: variation of the  $S_{21}$  amplitude with  $d/\lambda_0$  computed for different angles of incidence.

## III. RESULTS AND COMPARISON

In order to check if the unit-cells introduced in the previous section can be used successfully in a multibeam TA, two configurations have been designed. Both the planar transmitting surfaces are square, with a size  $D = 10\lambda_0$  and ratio  $F/D=0.9$ ,

where  $F$  is the focal distance between the feed and the TA surface. The feed is a vertically-polarized horn. The TAs are designed to have maximum radiation in the broadside direction.

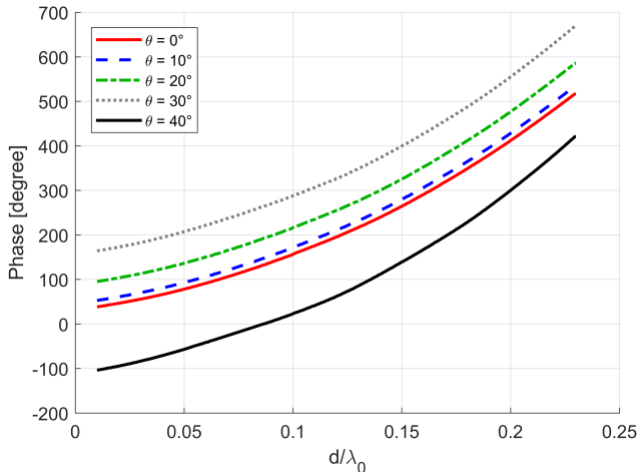


Fig. 5. Perforated dielectric unit-cell: variation of the  $S_{21}$  phase with  $d/\lambda_0$  computed for different angles of incidence.

Since the two unit-cells have not the same electrical size, for the realization of a  $10\lambda_0$  aperture it is necessary to use  $20 \times 20$  Malta-crosses, while the perforated dielectric TA is composed by  $40 \times 40$  elements.

At this preliminary stage, the different beams are obtained simply rotating the feed in the vertical plane of an angle  $\theta$  that varies between  $0^\circ$  and  $30^\circ$ . Because of the symmetry of the antenna, the same behavior for negative pointing angles is expected. The radiation patterns resulting from the simulation of the perforated dielectric TA for different position of the feed are plotted in Fig. 6. As the direction of maximum radiation deviates from the broadside, as the radiation performances degrade: the gain decreases, the main beam become larger and the side lobes increase. Nevertheless, it is worth to notice that in the angular region ( $0^\circ$ ,  $20^\circ$ ) the radiation patterns are quite good, with a limited reduction of the gain and deformation of the main beam.

In Table 1, the numerically computed values of the maximum gain obtained with the two transmitarrays in

TABLE I  
MULTIBEAM TAs GAIN COMPARISON

Angles	Gain (dB)	
	Malta-cross based TA	Perforated dielectric TA
$0^\circ$	27.5	27.2
$10^\circ$	25.2	27.2
$20^\circ$	24.7	26.5
$30^\circ$	22.3	25.1

correspondence of different pointing angles, are listed. From these results, it is evident that the Malta-cross based TA shows worse performances due to the stronger variation of the unit-cell behavior with the angle of incidence. Therefore, the gain

decreases faster, even if it has a higher value in the broadside direction. The greater dependence from the angle of arrival of the field radiated by the feed is confirmed by the radiation patterns shown in Fig. 7, related to the Malta-cross based TA. If compared with those in Fig. 6, it is possible to notice not only a faster reduction of the gain, but also a stronger deformation of the main beam and higher side lobes with respect to those affecting the pattern radiated by the perforated dielectric solution, that is less sensitive to the variation of the incidence angle: in fact, its radiation features from  $0^\circ$  to  $30^\circ$  remain almost good for all scanning angles.

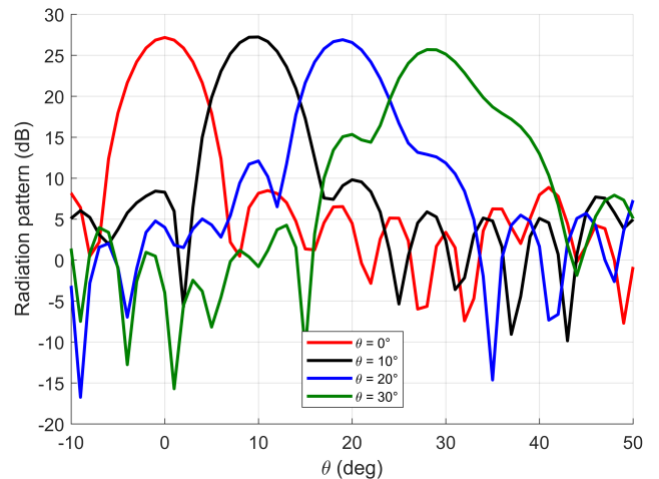


Fig. 6. Perforated dielectric TA: simulated radiation patterns in the E-plane for different angles of rotation of the feed.

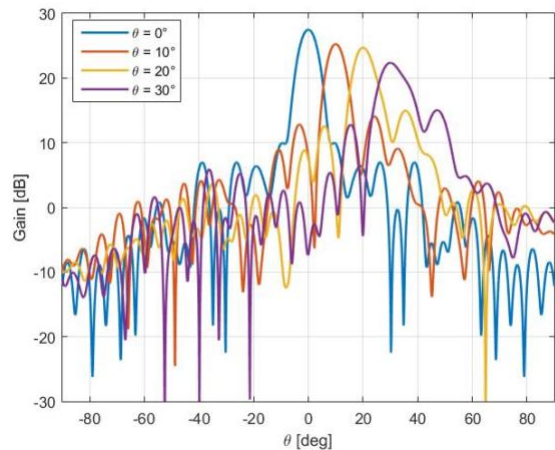


Fig. 7. Malta-cross based TA: simulated radiation patterns in the E-plane for different angles of rotation of the feed.

#### IV. CONCLUSION

In this paper, some preliminary results on the feasibility of a multibeam antennas configuration based on the use of a transmitarray are discussed. The design and numerical analysis of two, reduced size, structures prove that TAs are potentially

good candidates for this type of application. Nevertheless, some further optimization of the entire antenna, aimed to improve its radiation features, are necessary. Results on this aspect will be presented at the time of the conference.

## REFERENCES

- [1] J. G. Andrews *et al.*, "What will 5G be?," *IEEE J. Sel. Areas Commun.*, vol. 32, no. 6, pp. 1065–1082, Jun. 2014.
- [2] E. Dahlman, *et al.*, "5G wireless access: Requirements and realization," *IEEE Commun. Mag.*, vol. 52, no. 12, pp. 42–47, Dec. 2014.
- [3] T. L. Marzetta, "Noncooperative cellular wireless with unlimited numbers of base station antennas," *IEEE Trans. Wireless Commun.*, vol. 9, no. 11, pp. 3590–3600, Nov. 2010.
- [4] T. E. Bogale and L. B. Le, "Massive MIMO and mmWave for 5G wireless HetNet: Potential benefits and challenges," *IEEE Veh. Technol. Mag.*, vol. 11, no. 1, pp. 64–75, Mar. 2016.
- [5] E. G. Larsson, O. Edfors, F. Tufvesson, and T. L. Marzetta, "Massive MIMO for next generation wireless systems," *IEEE Commun. Mag.*, vol. 52, no. 2, pp. 186–195, Feb. 2014.
- [6] A. Swindlehursts, E. Ayanoglu, P. Heydari, F. Capolino, "Millimeter-wave massive MIMO: The next wireless revolution?," *IEEE Commun. Mag.*, vol. 52, no. 9, pp. 52–62, Sep. 2014.
- [7] Wei Hong, *et al.*, "Multibeam Antenna Technologies for 5G Wireless Communications," *IEEE Trans. Antennas Propag.*, vol. 65, no. 12, pp. 6231–6249, Dec. 2017.
- [8] A. H. Abdelrahman, F. Yang, A. Z. Esherbeni, and P. Nayeri, *Analysis and Design of Transmitarray Antennas*, M&C Publishers, 2017.
- [9] C. G. M. Ryan, *et al.*, "A wideband transmitarray using dual-resonant double square rings," *IEEE Trans. Antennas Propag.*, vol. 58, no. 5, pp. 1486–1493, May 2010.
- [10] A.-E. Mahmoud, W. Hong, Y. Zhang, and A. Kishk, "W-band multilayer perforated dielectric substrate lens," *IEEE Antennas Wireless Propag. Lett.*, vol. 13, pp. 734–737, 2014.
- [11] W. An, S. H. Xu, F. Yang, and M. K. Li, "A double-layer transmitarray antenna using Malta crosses with vias," *IEEE Trans. Antennas Propag.*, vol. 64, no. 3, pp. 1120–1125, Mar. 2016.
- [12] M. Jiang, Z. N. Chen, Y. Zhang, W. Hong, and X. Xuan, "Metamaterial-based thin planar lens antenna for spatial beamforming and multibeam massive MIMO," *IEEE Trans. Antennas Propag.*, vol. 65, no. 2, pp. 464–472, Feb. 2017.
- [13] A. H. Abdelrahman, A. Z. Elsherbeni, and F. Yang, "Transmission phase limit of multilayer frequency selective surfaces for transmitarray designs," *IEEE Trans. Antennas Propag.*, vol. 62, no. 2, pp. 690–697, Feb. 2014.
- [14] P. De Vita, A. Freni, G.L. Dassano, P. Pirinoli, R.E. Zich, "Broadband Element for High-Gain Single-Layer Printed Reflectarray Antenna", *Electronics Letters*, pp. 1247-1249, 2007.
- [15] A. Massaccesi, P. Pirinoli, "Enhancing the Bandwidth in Transmitarray Antennas Using Tapered Transmission Line Matching Approach," *12<sup>th</sup> European Conference on Antennas and propagation (EuCAP)*, London, UK, 2018